JOURNAL OF AIRCRAFT
Vol. 48, No. 1, January–February 2011

Comparative Study on Optimal Stiffener Placement for Curvilinearly Stiffened Panels

Manav Bhatia,* Rakesh K. Kapania,† and Dane Evans‡
Virginia Polytechnic Institute and State University, Blacksburg, Virginia 24061

DOI: 10.2514/1.C000234

Recent studies have shown that curved stiffeners offer potential for structural tailoring of metallic panels. However, the optimal placement of the stiffener curves has remained a challenge, due to both the presence of multiple local minima in the design space as well as the associated CPU cost to solve the problem. This paper presents two new approaches to design the stiffener curves by decomposition of the design space into size and shape variables. The approaches are built on a heuristic concept of effectiveness of a stiffener configuration, which argues that the most effective configuration will also provide the lowest optimized panel mass. The first approach estimates the best stiffener configuration, based purely on the first buckling mode of the unstiffened panel. The approach defines a heuristic metric for the effectiveness of a stiffener in increasing the buckling load capacity of a panel. The second approach uses optimization methods on both the sizing and shape variable subspaces. Mass is minimized over the sizing variable subspace, with constraint on buckling, while the buckling eigenvalue is maximized over the shape design variable subspace by varying the stiffener curves. The results are compared with optimization over a unified design space using a global optimization procedure, and it is shown that the proposed methods lead to better designs at lower CPU cost.

Nomenclature

f	=	function defining effectiveness metric
L	=	length of stiffener curve
M	=	effectiveness index of stiffener defined by curve $\boldsymbol{\phi}(\xi)$
p	=	scaling factor used in metric definition, dependent on applied stresses
$p_{\min}$, $p_{\max}$	=	minimum and maximum values of scaling factor, respectively
$w(x, y)$	=	displacement shape of first buckling mode of panel
θ	=	angle of stiffener segment with respect to x axis
ξ	=	nondimensional coordinate along stiffener curve
σ	=	applied stresses on panel boundary
σ_C	=	value of higher compressive principal stress, zero if neither σ_I or σ_{II} are compressive
σ_I, σ_{II}	=	principal stresses due to applied external loads
$\sigma_{\hat{n}_T}$	=	normal stress on surface defined by unit vector $\hat{n}_T$, calculated based on σ
$\boldsymbol{\phi}(\xi)$	=	curve defining (x, y) coordinate of stiffener along nondimensionalized coordinate ξ

I. Introduction

ONGOING revolution in information management, material science, computational science, and manufacturing technology has now made it possible to fabricate a new generation of mostly custom-built structures that will have a low part count, built-in multifunctionality, and an ability to tailor the structure according to the design requirements. Termed unitized structures, these structures are formed by adding or building up material, as opposed to subtractive (i.e., taking the material away, as in machining) or formative (casting) methods of manufacturing. For nearly three years, under a grant from NASA Langley Research Center in collaboration with Lockheed Martin, we have been developing a computer environment that will help the aerospace industry optimally design unitized structures, built using such approaches as the electron-beam free-form fabrication (EBF3), and will make use of the design flexibility (efficient use of geometry) and material placement made possible by these new manufacturing technologies.

The existing software for analysis and design of stiffened panels [1–5] uses analytical expressions or simplified discretization schemes to decompose the analysis methodology into specific failure modes. The failure modes include global buckling instability of the panel with the stiffeners, local buckling of the panel in between the stiffeners, and various modes of local buckling instability of the stiffeners themselves. The influence of mode switching on post-buckling behavior is also included, using simplified procedures for both analysis and design [6]. Specialized cost-effective analytical models are used to approximate the critical load for each of these failure modes. PASCO [1], PANDA [2,3], and VICONOPT [5] use gradient-based optimizers for the design of stiffened panels. The design variables include panel thickness, stiffener dimensions (depending on the kind of stiffener), and stiffener spacing, with user-selectable constraints for each kind of failure mode. There are two distinct advantages of this approach:

1) The analyses are highly cost effective, enabling evaluation of a large number of panel/stiffener concepts in a very short period of time.

2) Specialized models for each failure mode help in decomposition of the response functions, thereby making the optimization problems relatively well behaved. These models, however, should be used carefully and with good engineering judgement [7].

Another stiffened-panel design software, Hypersizer [8], uses similar simplified analysis procedures, but it also uses an optimization procedure based on permutations and combinations of both the continuous (stiffener dimensions and spacings, panel thickness, etc.) and discrete (stiffener concepts, etc.) variables. The inexpensive function evaluations make it possible to design stiffened panels based on such a combinatorial optimization scheme.

The readers are referred to Bedair [9] for a review of analysis methodology of stiffened plates and shells. Bedair emphasizes the influence of bending and torsional rigidity of the stiffeners on the resulting failure modes of a stiffened panel. As a result, different buckling modes become critical, as the stiffener dimensions are

Received 22 December 2009; revision received 25 October 2010; accepted for publication 25 October 2010.

*Postdoctoral Associate, Department of Aerospace and Ocean Engineering. Senior Member AIAA.

†Mitchell Professor, Department of Aerospace and Ocean Engineering. Associate Fellow AIAA.

‡Research Engineer, Department of Aerospace and Ocean Engineering.

varied for the same panel geometry. Additional references on analysis methodologies are given by Anderson and Stroud [1] and Bushnell [2,3]. Interested readers are also referred to work on topology optimization for stiffener placement [10,11] and design methods for curvilinear fiber placement for composite panels [12,13].

The present problem is that of variation of both the stiffener and panel cross-sectional dimensions and the stiffener geometries, such that they can follow curved paths on the panel. The analysis methodologies used in the aforementioned design codes for stiffened panels are specialized for straight stiffeners, and hence cannot be used for this purpose. Instead, a finite-element-based analysis and optimization framework are developed. The panel and the stiffeners are modeled using shell elements, and a buckling eigenvalue analysis gives the critical failure modes for the entire system, be it a global or a local mode of the panel or the stiffeners. The readers are referred to the paper by Gurav and Kapania [14] for details of the optimization framework. A direct challenge resulting from this approach is that all failure modes come out of a single analysis; hence, it is rather difficult to automatically decompose the limit state into individual modes as described earlier. Understandably, mode switching can occur as the stiffener dimensions and geometry are changed during optimization.

The problem definition here is to use high-fidelity finite element modeling to evaluate the panel buckling, stress, and crippling responses for a given loading and to find out the optimum stiffener curve and dimensions for minimum panel mass. This problem combines aspects of both shape and sizing optimization with multiple local minima.

Previous work on unitized structures by Kapania et al. [15] dealt with straight and curvilinear stiffeners with end points located a priori, for which only a sizing optimization was performed. Mulani et al. [16] developed an approach for optimal placement of stiffener end points, where only straight stiffeners were considered. A response surface (RS) of optimum stiffened-panel weight was constructed for different end point locations, and optimization using this RS gave the optimal end point locations. For two straight stiffeners, the construction of RS required 190 simulations. Although this algorithm could work with the global design space, with fewer chances of getting stuck in a local minimum, it was computationally very expensive for even a small subset of design parameters. Joshi et al. [17] extended this approach to include the stiffener curvature as a design variable. Despite these advances, the primary challenge of high computational expense remained.

This paper develops a heuristic approach toward this problem by introducing a concept of effectiveness of the stiffener configuration, which is discussed in detail in the next section. This concept is used to develop two new approaches for optimization where the problem is decomposed into two parts: the first part involves calculation of the best stiffener curve that would give the lowest mass of the panel, and the second step involves a sizing optimization while keeping the stiffener curve constant. The first approach develops a metric for the effectiveness of a stiffener curve based purely on the first buckling mode of the unstiffened panel. Using the notion of stiffener effectiveness, the second approach identifies that, out of a set of stiffener configurations with constant cross section, the one with the highest panel-buckling eigenvalue is the most effective. This is then translated into an optimization problem where the cross section of the stiffeners is held constant, and the shape is varied to maximize the buckling eigenvalue. The resulting shape is then sized to achieve minimum mass. Results are presented for optimization of panels with one and two stiffeners, and the latter is compared with results from global optimization over the unified design space, with both shape and sizing design variables.

Section II presents the formulation of the approach, followed by results in Sec. III, and conclusions are listed in Sec. IV.

II. Formulation

A. Stiffener Effectiveness Metric

A heuristic method, called the stiffener effectiveness approach (SEA), is developed and detailed here. The basis of this approach comes from a fundamental understanding that the limit-buckling load of a panel is a combination of its geometry and the loads acting on the panel. The geometry is collectively defined by the cross-sectional dimensions of the panel and stiffeners and the geometry of the stiffener curves.

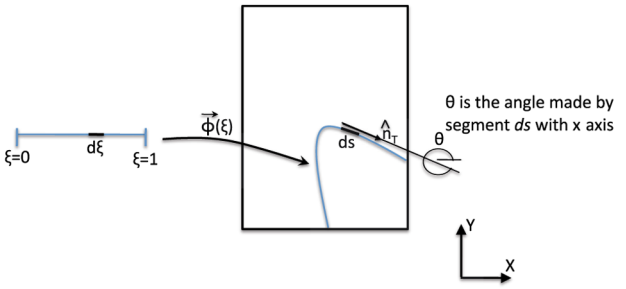

Fig. 2 Stiffener mapping from nondimensional one-dimensional ξ space to physical space on the panel.

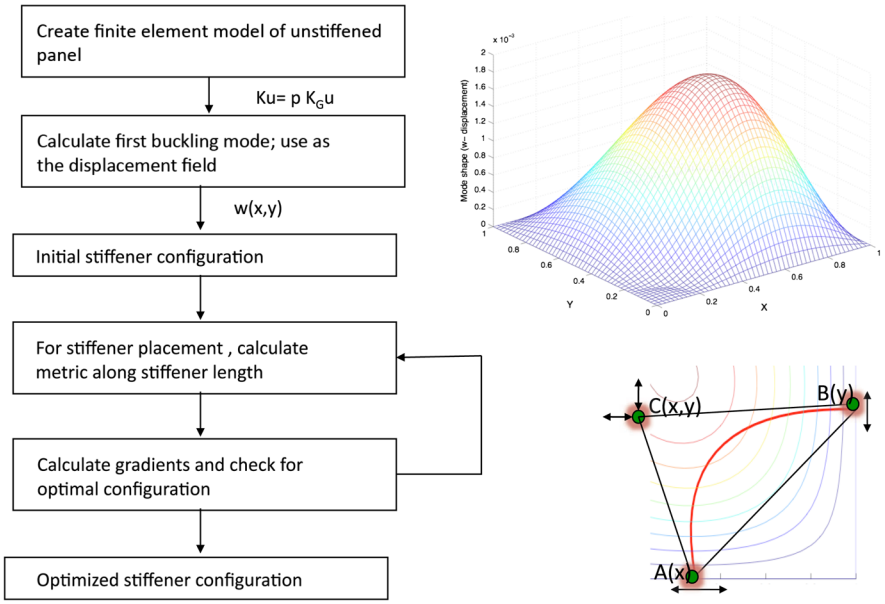

Fig. 1 SEA flowchart.

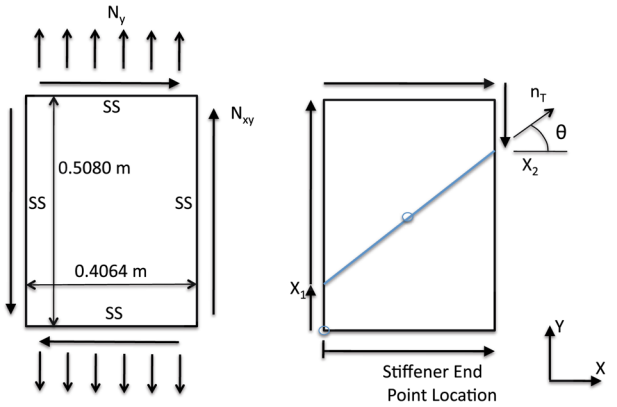

Fig. 3 Panel dimensions and sign convention for positive loads and stiffener orientation angle.

The following discussion first presents a rationale behind the concept and then proposes a formulation for the effectiveness metric.

The primary purpose of a stiffener is to increase the buckling load of a panel. For an unstiffened panel, the most critical mode to be prevented is the first buckling mode, which is different for each loading and boundary condition on the panel. Hence, there is some information in the buckling mode that can perhaps be used to find an optimal location of the stiffener. In the formulation presented next, the first buckling mode is used as the displacement field $w(x, y)$, which is defined over the entire domain of the panel and is obtained from a linearized buckling eigenvalue analysis.

In this paper, the effectiveness of a stiffener is treated as a measurable quantity, such that a stiffener configuration with a higher value of the effectiveness metric will have a higher panel-buckling load. As a corollary, a stiffener configuration with a higher effectiveness metric will result in a lower structural mass when sized with buckling constraints. The following discussion identifies a few important parameters that influence the effectiveness of a stiffener configuration, and then it proposes an expression to quantify an effectiveness metric [Eq. (2)]. It is argued that the effectiveness metric depends on both the location and orientation of stiffeners on the panel.

For instance, consider a square, simply supported panel under biaxial compression that is known to have a critical buckling mode defined by a half-sine wave. Consider two stiffener curves: the first curve is defined to run close to the boundary of the panel, and the second curve is defined to be along one of the panel diagonals. Let the effectiveness metric be defined as the integration of displacement squared along the stiffener per unit length [defined later in Eq. (9)]. This will have a small value for the first stiffener curve, hence a small effectiveness. Similarly, integration of displacement squared per unit length along the second stiffener will return a much higher value, hence a higher effectiveness. It is intuitive that if the two stiffeners have the same cross-sectional dimensions, then the second configuration will have a higher buckling load than the first. Hence, the metric can be related to the effectiveness of a stiffener in increasing the buckling load, and it is dependent on the absolute value of the transverse displacement component of the buckling mode.

As a second example, consider a simply supported circular plate of radius R under radial compression. The first buckling mode for such a

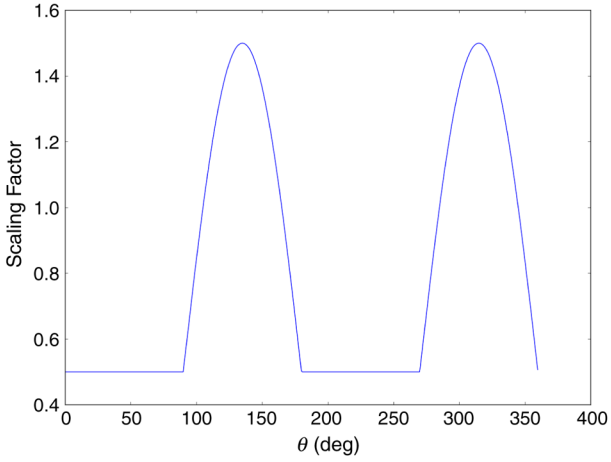

a) Load case 1: pure shear

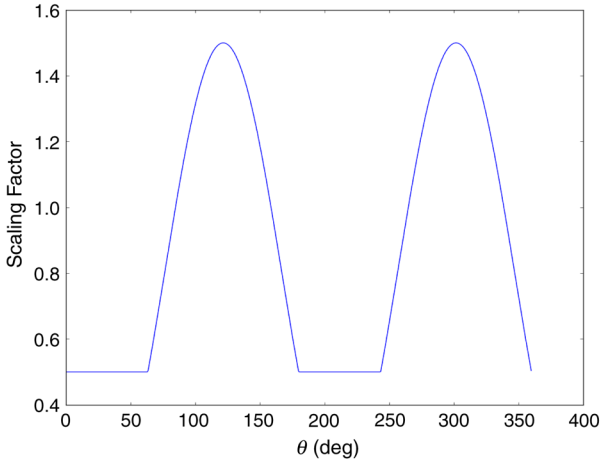

b) Load case 2: combined shear and compression, N_y/N_{xy} = 1.0

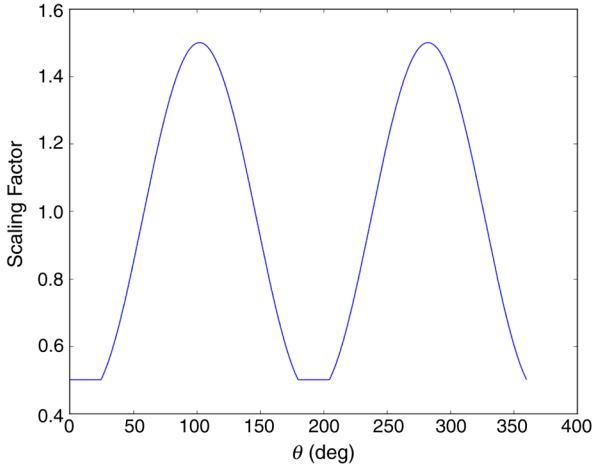

c) Load case 3: combined shear and compression, N_y/N_{xy} = 4.35

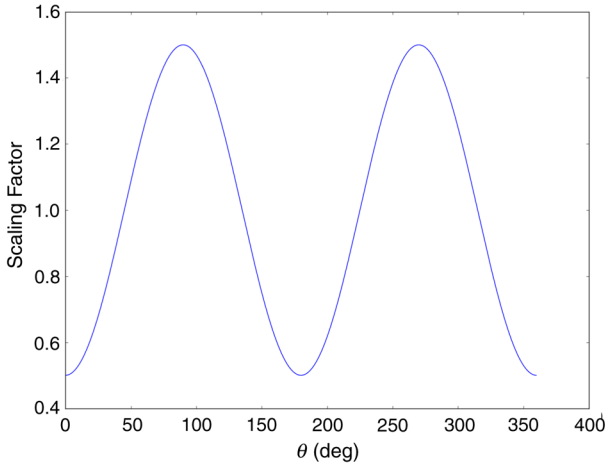

d) Load case 4: pure compression

Fig. 4 Scaling factor for different load cases.

plate is axisymmetric, with a circumferential nodal line at the plate boundary. Consider two stiffener curves: first, as a circle of some radius centered at $r = 0$, and second, as a diametric stiffener cutting across the modal contour lines. Using the transverse displacement component of the first buckling mode as the displacement field, the effectiveness metric is defined as integration of the displacement gradient squared per unit length along the two stiffener curves [defined later in Eq. (10)]. The value of this metric will be zero for the first curve and a finite value for the second. Hence, the metric of the second stiffener is higher than that of the first curve, and this is consistent with studies that have indicated that a diametrically stiffened circular plate has a higher buckling load than a ring-stiffened circular plate for the same stiffener dimensions [18,19]. Wang and Wang [18] assumed the stiffener to be rigid by applying a simply supported boundary condition at the location of the ring stiffener, and they were able to show an increment of buckling eigenvalue from 4.2 to about 5.3 for a simply supported plate ($\lambda = 0.3$ in Fig. 1). Barik [19] (table 5.6, pp. 207) studied the case of a diametrically stiffened plate and was able to show that the buckling capacity increased from 4.2 to 13.19 with the increasing stiffener rigidity ratio.

This suggests that if stiffeners are placed right along the contours of the critical buckling mode shape of the panel, they will provide little gain in load capacity of the panel. In fact, the stiffeners will be most effective if they run normal to these contours or, in other words, along the gradient of the panel modal contours.

A third, and important, consideration is that of the direction of principal compressive stress, which defines the favorable direction of stiffener path (i.e., a stiffener placed along this direction would have a higher effectiveness).

Taking these three points into consideration, a stiffener effectiveness metric is proposed in Eq. (2). The ability to quantify the effectiveness allows the use of an optimization algorithm to find the most effective curve, and a procedure is proposed in Fig. 1. The stiffener shape parametrization and calculation of metric values are discussed here, and the procedure for stiffener placement based on these metrics is elaborated in Sec. II.B.

As shown in Fig. 1, the stiffener shape is represented as a curve with three control points: A, B, and C. Control points A and C always lie on the panel edges (Fig. 2), and their locations are defined by one parameter each, measured along the perimeter on the panel (see Fig. 3). Location of the third control point, C, is defined using its x

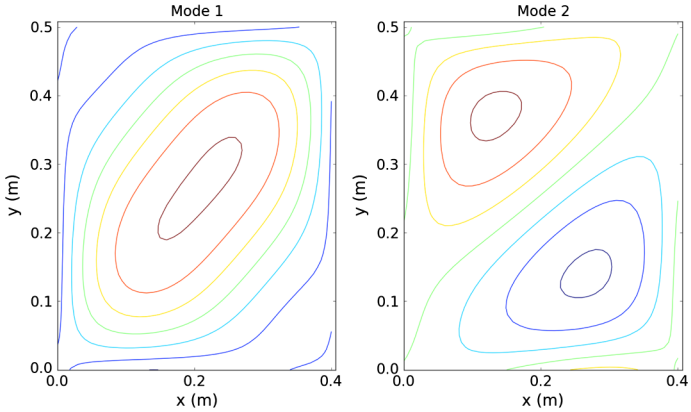

a) First and second buckling mode shapes

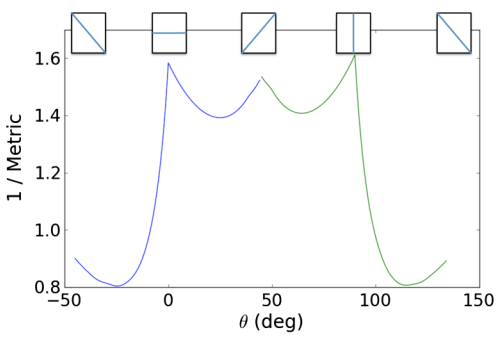

b) Integrated displacement per unit length along stiffener [Eq (9)]

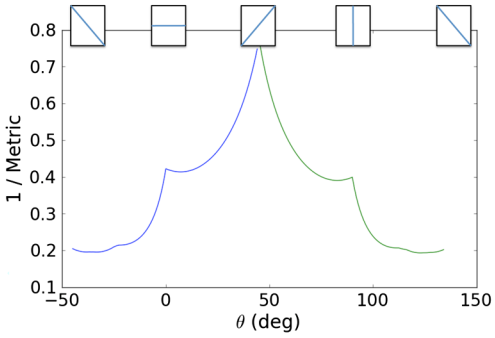

c) Integrated displacement gradient per unit length along stiffener [Eq (10)]

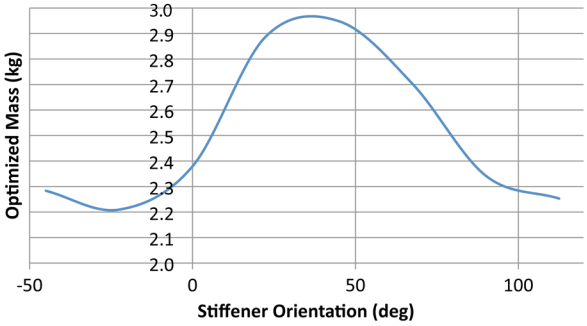

d) Optimized structural mass for stiffener configurations at various angles

Fig. 5 Plot of inverse of stiffener effectiveness metrics with respect to stiffener orientation: load case 1 (pure shear).

and y coordinates. Hence, a total of four design variables are needed to control the shape of the stiffener curve. Let $\boldsymbol{\phi}(\xi)$ be the stiffener curve based on these control points and defined along the nondimensional coordinate ξ of the stiffener. Hence, the function $\boldsymbol{\phi}(\xi)$ maps each ξ point of the curve to a unique (x, y) location within the panel boundaries. This is shown in Fig. 2:

$$\boldsymbol{\phi}(\xi) = \phi_x(\xi)\hat{i} + \phi_y(\xi)\hat{j} \tag{1}$$

where $\phi_x(\xi)$ and $\phi_y(\xi)$ are functions describing the x and y coordinates of the stiffener curve.

It is assumed that the stiffener is made from a homogenous material. Let the length of stiffener curve $\boldsymbol{\phi}(\xi)$ be denoted as L and the panel displacement field be $w(x, y)$. Then, the metric $M[w(x, y), \boldsymbol{\phi}(\xi)]$ is defined as

$$M[w(x,y),\boldsymbol{\phi}(\xi)] = \int_0^L f[w(x,y),\boldsymbol{\phi}(\xi)]\,\mathrm{d}s = \int_0^1 f[w(x,y),\boldsymbol{\phi}(\xi)]\frac{\mathrm{d}s}{\mathrm{d}\xi}\,\mathrm{d}\xi \tag{2}$$

where $\mathrm{d}s$ is the length of an element of the stiffener curve $\mathrm{d}\boldsymbol{\phi}$, and the function $f[w(x, y), \boldsymbol{\phi}(\xi)]$ can be appropriately chosen to define the dependence of the metric on the displacement field [Eqs. (9) and (10)]. The stiffener curve element is written as

$$\mathrm{d}\boldsymbol{\phi}(\xi) = \left(\frac{\mathrm{d}\phi_x(\xi)}{\mathrm{d}\xi}\hat{i} + \frac{\mathrm{d}\phi_y(\xi)}{\mathrm{d}\xi}\hat{j}\right)\mathrm{d}\xi \tag{3}$$

$$\mathrm{d}s = \sqrt{\mathrm{d}\boldsymbol{\phi}(\xi)\cdot\mathrm{d}\boldsymbol{\phi}(\xi)} = \sqrt{\left(\frac{\mathrm{d}\phi_x(\xi)}{\mathrm{d}\xi}\right)^2 + \left(\frac{\mathrm{d}\phi_y(\xi)}{\mathrm{d}\xi}\right)^2}\,\mathrm{d}\xi \tag{4}$$

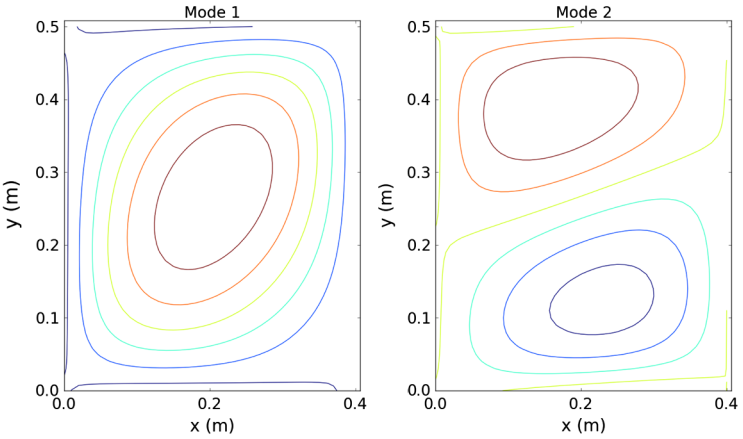

a) First and second buckling mode shapes

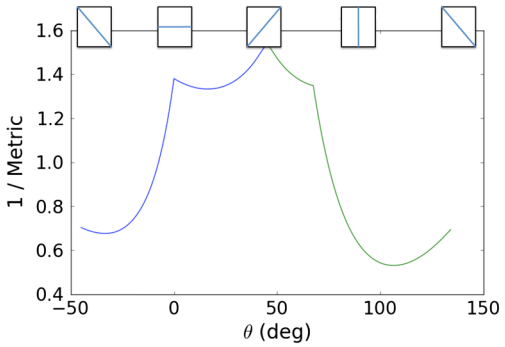

b) Integrated displacement per unit length along stiffener [Eq (9)]

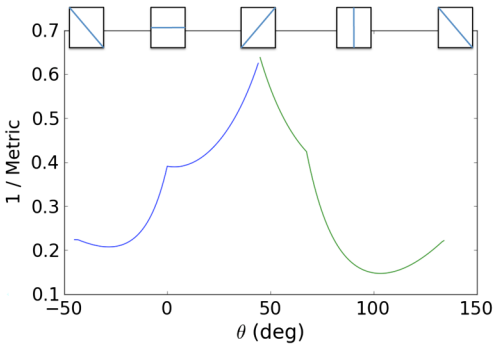

c) Integrated displacement gradient per unit length along stiffener [Eq (10)]

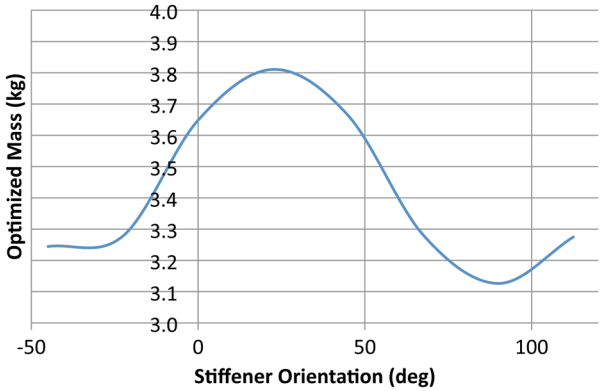

d) Optimized structural mass for stiffener configurations at various angles

Fig. 6 Plot of inverse of stiffener effectiveness metrics with respect to stiffener orientation: load case 2 ($N_y/N_{xy} = 1.0$).

and, L is the length of the stiffener curve that is measured by the following integral along the length of the stiffener curve:

$$L = \int_0^1 \frac{\mathrm{d}s}{\mathrm{d}\xi}\,\mathrm{d}\xi = \int_0^1 \sqrt{\left(\frac{\mathrm{d}\phi_x(\xi)}{\mathrm{d}\xi}\right)^2 + \left(\frac{\mathrm{d}\phi_y(\xi)}{\mathrm{d}\xi}\right)^2}\,\mathrm{d}\xi \tag{5}$$

The metric M is a measure of how well a given stiffener, defined by the curve $\boldsymbol{\phi}(\xi)$, performs for the given load case. Hence, with an appropriate definition of this metric, an optimization problem can be defined such that the metric M is to be maximized by varying the geometric curve $\boldsymbol{\phi}(\xi)$ using its control points A, B, and C. The present work uses a third-order B-spline representation with three control points and a knot vector of $\{0, 0, 0, 1, 1, 1\}$. The knot vectors are used to calculate the parametric B-spline shape functions $N_{i,3}(\xi)$ corresponding to the ith control point [20] ($i = 1$ for point A, $i = 2$ for point B, and $i = 3$ for point C). With the definition of the shape functions and the known control point locations $\mathbf{X}_i$, the stiffener curve is defined as

$$\boldsymbol{\phi}(\xi) = N_{1,3}\mathbf{X}_1 + N_{2,3}\mathbf{X}_2 + N_{3,3}\mathbf{X}_2 \tag{6}$$

Let $\hat{n}_T$ be a tangential unit vector to the stiffener curve at location ξ along the curve (see Fig. 2), such that

$$\hat{n}_T = \frac{\mathrm{d}\boldsymbol{\phi}(\xi)}{\mathrm{d}s} \tag{7}$$

Let the displacement measured along the stiffener length be represented as $\tilde{w}[\boldsymbol{\phi}(\xi)]$, such that

$$\tilde{w}[\boldsymbol{\phi}(\xi)] = w[\phi_x(\xi), \phi_y(\xi)] \tag{8}$$

The problem then depends on the appropriate definition of the function $f\{\tilde{w}[\boldsymbol{\phi}(\xi)], \boldsymbol{\phi}(\xi)\}$. Two different functions are studied here:

$$f^{(1)}\{\tilde{w}[\boldsymbol{\phi}(\xi)], \boldsymbol{\phi}(\xi)\} = p(\sigma, \hat{n}_T)\,\frac{\tilde{w}^2[\boldsymbol{\phi}(\xi)]}{L} \tag{9}$$

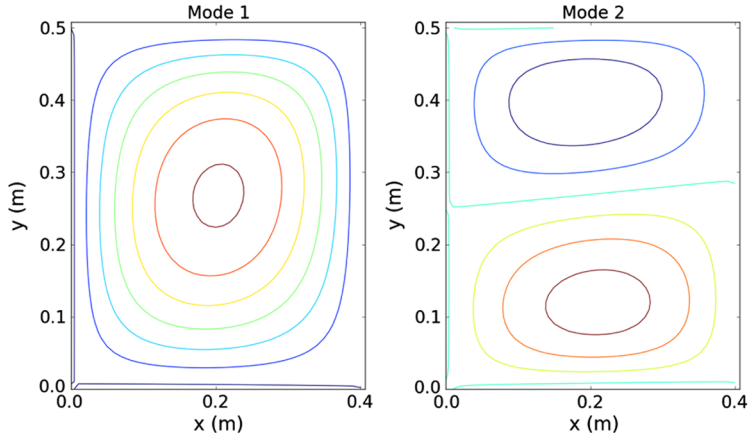

a) First and second buckling mode shapes

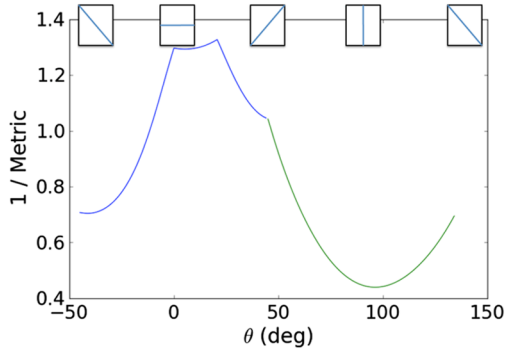

b) Ingegrated displacement per unit length along stiffener [Eq (9)]

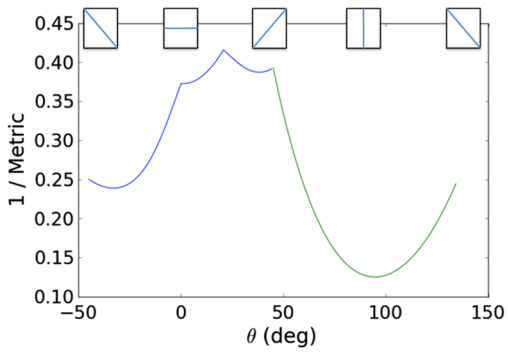

c) Integrated displacement gradient per unit length along stiffener [Eq (10)]

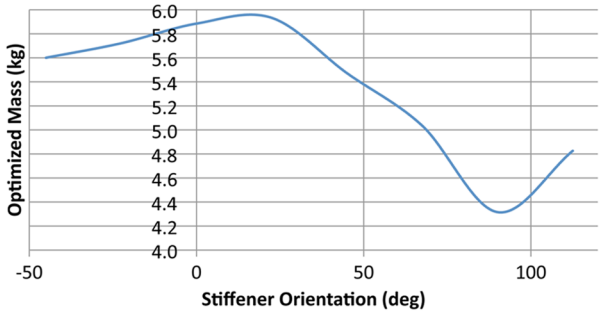

d) Optimized structural mass for stiffener configurations at various angles

Fig. 7 Plot of inverse of stiffener effectiveness metrics with respect to stiffener orientation: load case 3 ($N_y/N_{xy} = 4.35$).

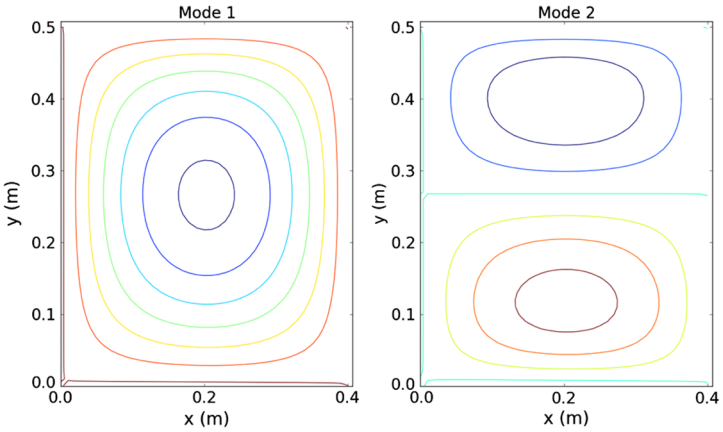

a) First and second buckling mode shapes

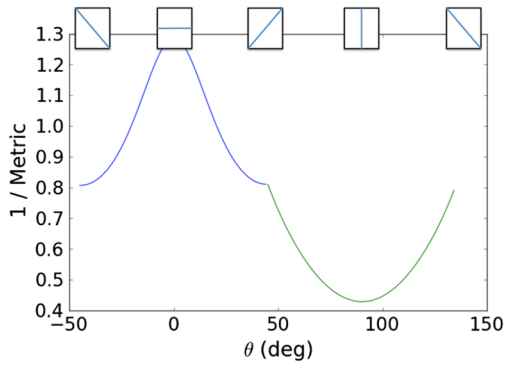

b) Integrated displacement per unit length along stiffener [Eq (9)]

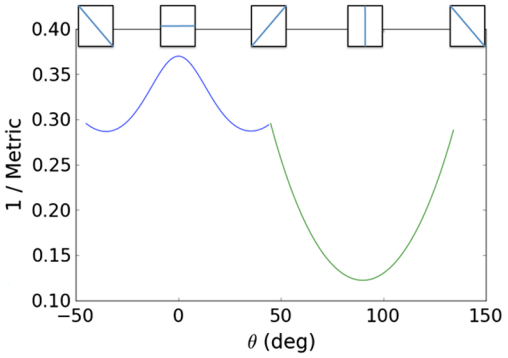

c) Integrated displacement gradient per unit length along stiffener [Eq (10)]

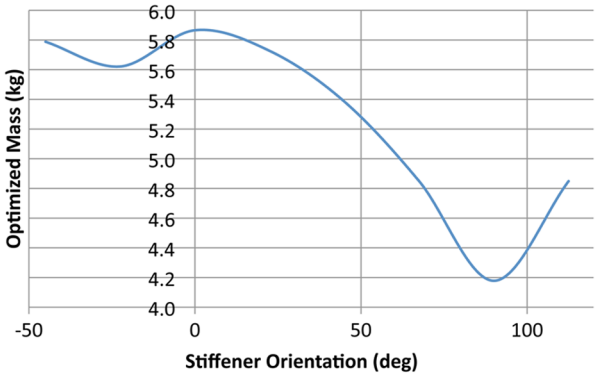

d) Optimized structural mass for stiffener configurations at various angles

Fig. 8 Plot of inverse of stiffener effectiveness metrics with respect to stiffener orientation: load case 4 ($N_y/N_{xy} = \infty$).

$$f^{(2)}\{\tilde{w}[\boldsymbol{\phi}(\xi)], \boldsymbol{\phi}(\xi)\} = p(\sigma, \hat{n}_T)\frac{\{\nabla\tilde{w}[\boldsymbol{\phi}(\xi)]\cdot\hat{n}_T\}^2}{L} \tag{10}$$

The scaling factor $p(\sigma, \hat{n}_T)$ is defined based on the orientation of the stiffener curve and the direction of maximum compressive principal stress. This is taken into account through the definition of a reference stress σ_C, which depends on the magnitude of the principal stresses σ_I and σ_{II}:

$$\sigma_C = \begin{cases} \min(\sigma_I, \sigma_{II}) & \text{if } \sigma_I < 0 \quad \text{or} \quad \sigma_{II} < 0 \\ 0 & \text{if } \sigma_I, \sigma_{II} > 0 \end{cases} \tag{11}$$

In situations where the panel loading does not produce a compressive stress in any direction, a stiffener placement would not be influenced by buckling considerations, and all directions are weighted equally by a factor $p_{\min}$ [Eq. (12)]. Similarly, when the stiffener segment is in the direction where the normal stress component is tensile in nature, the factor is assumed to be $p_{\min}$ [Eq. (13)]. In all other cases, the magnitude of compressive stress along the stiffener segment orientation is used to calculate the scaling factor [Eq. (14)]. Thus, this weighting scheme results in creating a preference for the direction of compression, and it is summarized as

$$p(\sigma, \hat{n}_T) = p_{\min}, \qquad \sigma_C = 0 \tag{12}$$

$$p(\sigma, \hat{n}_T) = p_{\min}, \qquad \sigma_{\hat{n}_T} > 0 \tag{13}$$

Table 1 Material properties

Property	Value
Young's modulus, GPa	73.085
Poisson's ratio	0.33
Maximum yield stress, MPa	468.84

Table 2 Design variables used in optimization[a]

Name	Used in SEA	Used in PSO-straight	Used in PSO-curved	Used in combined PSO-unified	Lower bound	Upper bound
Stiffener 1: beginning point	No	Step 1	Step 1	Yes	0.01	0.9144
Stiffener 1: end point	No	Step 1	Step 1	Yes	0.01	0.9144
Stiffener 2: beginning point	No	Step 1	Step 1	Yes	0.9144	1.8188
Stiffener 2: end point	No	Step 1	Step 1	Yes	0.9144	1.8188
Stiffener 1: angle, °	No	No	Step 1	Yes	−20	20
Stiffener 2: angle, °	No	No	Step 1	Yes	−20	20
Stiffener 1: height, m	Yes	Step 2	Step 2	Yes	0.01	0.05
Stiffener 2: height, m	Yes	Step 2	Step 2	Yes	0.01	0.05
Stiffener 1: thickness, m	Yes	Step 2	Step 2	Yes	0.001	0.05
Stiffener 2: thickness, m	Yes	Step 2	Step 2	Yes	0.001	0.05
Panel thickness, m	Yes	Step 2	Step 2	Yes	0.001	0.05

[a]Same bounds used for all cases. Beginning and end points are measured clockwise along the perimeter of the panel, starting from the lower left corner.

Table 3 Optimum mass obtained using the two approaches[a]

				SEA		PSO-straight		PSO-curved		PSO-unified	
Load case	N_{xy}, kN/m	N_y, kN/m	N_y/N_{xy}	Mass, kg	Time, min.	Mass, kg	Time, min.	Mass, kg	Time, min.	Mass, kg	Time, min.
1	0.0	−1313.45	$-\infty$	2.995	10	2.884	106	2.904	88	3.373	213
2	106.126	−462.333	−4.36	2.012	17	1.976	90	1.972	88	2.295	97
3	96.319	−376.521	−3.91	2.013	5	1.872	75	1.832	88	2.328	122
4	201.395	−227.664	−1.13	1.861	14	1.760	46	1.707	88	1.970	132
5	711.53	0.0	0.0	1.824	15	1.914	93	2.151	88	2.194	649

[a]Computations performed on computer with dual four-core 3.0 GHz Intel Xeon processors (eight cores) and 20 GB RAM.

$$p(\sigma, \hat{n}_T) = p_{\min} + p_{\max} \frac{|\sigma_{\hat{n}_T}|}{|\sigma_C|}, \qquad \sigma_C, \sigma_{\hat{n}_T} < 0 \tag{14}$$

where $p_{\min}$ and $p_{\max}$ are assumed to be 0.5 and 1.0, respectively, in this work, and $\sigma_{\hat{n}_T}$ is calculated from the plane stress transformation relations:

$$\sigma_{\hat{n}_T} = \sigma_x \cos^2(\theta) + \sigma_y \sin^2(\theta) + \sigma_{xy} \sin(2\theta) \tag{15}$$

for the applied loads σ_x, σ_y, and σ_{xy}. As shown in Fig. 2, the angle θ is defined as that created by the stiffener segment unit vector with the x axis. Plots of the scaling factor for different load cases, shown in Fig. 4, are discussed in the next section.

B. Stiffener Placement

1. *Placement Based on Effectiveness Metric: One Stiffener*

It is important to note that the metric defined in the previous section is based on a single stiffener curve.

For a single stiffener, the goal is to find a curve with the highest value of the metric. This can be defined as an optimization problem for a given loading condition:

$$\max M[w(x, y), \boldsymbol{\phi}(\xi, X)] \tag{16}$$

where X are the design variables for the control point locations of the stiffeners (shown as double-sided arrows in Fig. 1). The overall approach to optimization is shown in Fig. 1. Once the critical buckling mode shape is obtained for an unstiffened panel (upper right-hand figure), the optimization problem is used to maximize the effectiveness index, M, on this displacement field $w(x, y)$. The present work uses finite differencing to calculate the gradient of the metric function. The stiffener curve obtained from this procedure can then be used for sizing optimization to calculate the minimum mass of the stiffened panel subject to constraints on the buckling eigenvalue, von Mises stress, and stiffener crippling stress.

2. *Placement Based on Effectiveness Metric: Two Stiffeners*

For placement of two stiffeners, the procedure described in Sec. II.B.1 gives a single stiffener curve, which is used as a basis to

Table 4 Design variables values for load case 1

Stiff. No./Name	SEA	PSO-straight	PSO-curved	PSO-unified
1/beginning point	0.62992	0.7639	0.64980	0.0100
1/end point	1.69672	1.5636	1.6873	0.9405
2/beginning point	0.78232	0.6489	0.7853	0.6724
2/end point	1.54432	1.6784	1.5504	1.5846
1/angle, °	0.0	0.0	2.01	6.37
2/angle, °	0.0	0.0	−3.7	0.77
1/height, m	0.0373	0.05	0.0408	0.0310
2/height, m	0.0400	0.0448	0.408	0.0500
1/thickness, m	0.0046	0.00194	0.0033	0.0018
2/thickness, m	0.0038	0.00185	0.0033	0.0029
		Panel values		
Mass, kg	2.995	2.884	2.904	3.373
Thickness, m	0.0044	0.0046	0.0043	0.0053
		Constraints		
Buckling	1.0147	0.9993	1.003	1.001
von Mises stress	0.6459	0.6340	0.651	0.603
Crippling	0.5993	0.9630	0.995	0.753

Table 5 Design variable values for load case 2

Stiff. No./Name	SEA	PSO-straight	PSO-curved	PSO-unified
1/beginning point	0.6196	0.6301	0.6495	0.6456
1/end point	1.64592	1.6695	1.6937	1.5242
2/beginning point	0.7415	0.7578	0.7778	0.8988
2/end point	1.524	1.5457	1.5632	1.7342
1/angle, °	0.0	0.0	0.72	0.78
2/angle, °	0.0	0.0	−1.01	−19.94
1/height, m	0.0405	0.0489	0.0386	0.0414
2/height, m	0.0395	0.04116	0.0386	0.0239
1/thickness, m	0.0012	0.001	0.0013	0.0028
2/thickness, m	0.0013	0.001	0.0013	0.0014
		Panel values		
Mass, kg	2.012	1.976	1.972	2.284
Thickness, m	0.0032	0.0032	0.0032	0.0036
		Constraints		
Buckling	0.9930	0.9998	1.002	0.999
von Mises Stress	0.3326	0.3361	0.337	0.321
Crippling	0.5833	0.7921	0.988	0.315

Table 6 Design variables values for load case 3

Stiff. No./Name	SEA	PSO-straight	PSO-curved	PSO-unified
1/beginning point	0.62992	0.7498	0.7763	0.1711
1/end point	1.66624	1.5191	1.5563	1.7081
2/beginning point	0.75184	0.6457	0.6425	0.6917
2/end point	1.54432	1.6817	1.6899	1.5888
1/angle, °	0.0	0.0	0.87	−13.86
2/angle, °	0.0	0.0	0.32	0.45
1/height, m	0.0231	0.05	0.0391	0.0100
2/height, m	0.0251	0.0399	0.0391	0.0500
1/thickness, m	0.0051	0.001	0.0011	0.0050
2/thickness, m	0.0046	0.001	0.0011	0.0010
		Panel values		
Mass, kg	2.013	1.872	1.832	2.328
Thickness, m	0.0029	0.00302	0.0029	0.0039
		Constraints		
Buckling	1.0070	1.003	1.001	1.003
von Mises stress	0.3326	0.2943	0.298	0.258
Crippling	0.5833	0.7093	0.989	0.589

Table 7 Design variables values for load case 4

Stiff. No./Name	SEA	PSO-straight	PSO-curved	PSO-unified
1/beginning point	0.61976	0.7607	1.2178	0.5960
1/end point	1.66624	1.5084	0.1577	1.5325
2/beginning point	0.75184	0.5946	1.0728	0.7832
2/end point	1.53416	1.6723	0.3035	1.8148
1/angle, °	0.0	0.0	0.7	−1.00
2/angle, °	0.0	0.0	−0.2	20.00
1/height, m	0.0299	0.0491	0.0451	0.0426
2/height, m	0.0284	0.0478	0.0451	0.0454
1/thickness, m	0.0022	0.001	0.001	0.0013
2/thickness, m	0.0025	0.001	0.001	0.0010
		Panel values		
Mass, kg	1.861	1.760	1.707	1.970
Thickness, m	0.0029	0.0028	0.0027	0.0031
		Constraints		
Buckling	1.026	0.9992	1.003	1.002
von Mises stress	0.3258	0.3236	0.329	0.295
Crippling	0.2021	0.5196	0.999	0.777

create multiple curves. This base curve is copied and placed at two locations, such that the midline of the panel is divided into three equal portions. This stiffener shape is held constant for mass minimization, subject to constraints on buckling eigenvalue, von Mises stress, and stiffener crippling stress. This approach uses a gradient-based optimizer for mass minimization, and the approach is termed as SEA in the results presented in Sec. III.B.

Table 8 Design variables values for load case 5

Stiff. No./Name	SEA	PSO-straight	PSO-curved	PSO-unified
1/beginning point	0.3230	0.6761	0.4572	0.4686
1/end point	1.5058	1.2880	1.5735	1.1630
2/beginning point	0.5914	0.3627	0.6607	0.3682
2/end point	1.2374	1.5527	1.3716	1.5002
1/angle, °	0.0	0.0	1.83	0.36
2/angle, °	0.0	0.0	−1.36	−1.24
1/height, m	0.0408	0.0393	0.0316	0.0412
2/height, m	0.0274	0.0387	0.0316	0.0309
1/thickness, m	0.0012	0.001	0.0026	0.0014
2/thickness, m	0.0019	0.001	0.0026	0.0021
		Panel values		
Mass, kg	1.824	1.914	2.151	2.194
Thickness, m	0.0029	0.00314	0.0033	0.0035
		Constraints		
Buckling	1.006	0.9976	1.001	1.001
von Mises stress	0.6813	0.633	0.9926	0.991
Crippling	0.8356	0.962	1.002	0.992

3. Two-Step Particle Swarm Optimization Approach

Optimization is used on the two decomposed shape and sizing variable subspaces. The most effective stiffener curves are obtained in the shape variable subspace by solving a bound unconstrained optimization problem for maximization of the buckling eigenvalue. Only the stiffener curve shape variables are allowed to change, while the stiffener and panel cross sections are held constant. Upon convergence, the curve is held constant, and the cross-sectional dimensions are sized for minimum mass subject to constraints on buckling eigenvalue, von Mises stress, and stiffener crippling stress. A particle swarm optimization (PSO) [21] algorithm is used for these results.

This approach is used to obtain two sets of results: one where the stiffeners are kept straight, and the other where they are allowed to have a curvature. The former is called PSO-straight, the latter is called PSO-curved.

III. Results

Two sets of results are presented in this section. As mentioned earlier, a stiffener configuration with high metric value is expected to result in a lower optimized panel mass. With this perspective, the performance of the two metric definitions is compared for a panel with one stiffener under four different load cases. These results are presented in Sec. III.A. The next set of results, presented in Sec. III.B, compares minimum mass designs from four different optimization approaches. All optimizations for mass minimization have constraints on buckling eigenvalue, von Mises stress, and crippling stress for the stiffeners.

All panel analyses, with or without stiffeners, are performed with NASTRAN using CTRIA3 shell finite element. The stiffened-panel geometry and mesh are regenerated for each design point analysis during optimization. The details of this approach can be found in the paper by Gurav and Kapania [14].

A. Simply Supported Rectangular Panel: Single Stiffener

A simply supported rectangular panel of size 0.4064×0.5080 m (Fig. 3) and material properties listed in Table 1 is studied under four different load cases: 1) pure shear, $N_y = 0$ and $N_{xy} = 462$ kN/m; 2) equal shear and compression, $N_y = -462$ kN/m and $N_{xy} = 462$ kN/m; 3) combined shear and compression with dominant compression, $N_y = 2009.7$ kN/m and $N_{xy} = 462$ kN/m; and 4) uniaxial compression, $N_y = 2009.7$ kN/m and $N_y = 0$ kN/m.

For the results presented in this section, the stiffener is kept straight, and its midpoint is constrained to lie at the center of the panel (see Fig. 3). The metrics are studied for different orientations of the stiffener. The scaling factor [Eqs. (12–14)] are plotted for each load case in Fig. 4. These plots for each load case show that, for angles where the component of stress is positive, the value is limited to $p_{\min}$ (chosen as 0.5 here); otherwise, it is calculated based on the stress component along θ. For pure shear (load case 1, Fig. 4a), the two principal stresses are tensile and compressive in nature along $+45$ and $-45°$, respectively. For a pure compressive load (load case 4, Fig. 4d), no value of θ has a tensile component; hence, the scaling factor varies as the principal stress with different stiffener orientation. As expected, the scaling factor at any angle θ is equal to the value at $\theta + 180°$.

The purpose of this study is to identify whether the effectiveness metric value calculated based on the first buckling mode shape can mimic the variation of minimum mass for different stiffener orientations.

The first two buckling mode shapes of the unstiffened panel for each load case are shown in Figs. 5a, 6a, 7a, and 8a, respectively. It is important to note that the buckling mode shapes are of primary interest here, and the buckling load factors of the unstiffened panel do not contribute to the analysis. Hence, these mode shapes can be generated using an arbitrary thickness for the panel. The scaling factor and mode shapes are together used to calculate the metric function values for stiffener curves.

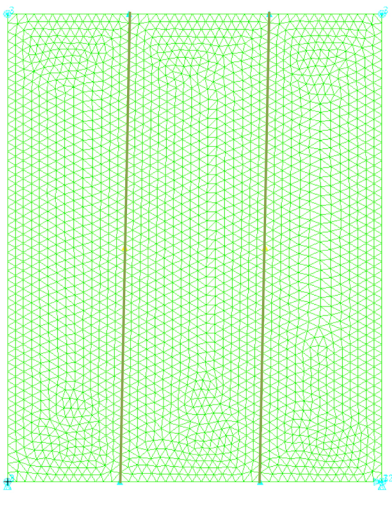

a) Stiffener effectiveness approach: 2.995 kg

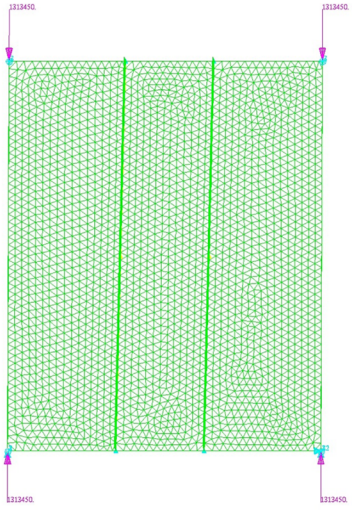

b) PSO-straight: 2.884 kg

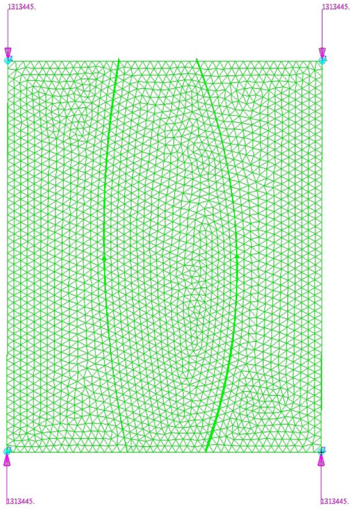

c) PSO-curved: 2.904 kg

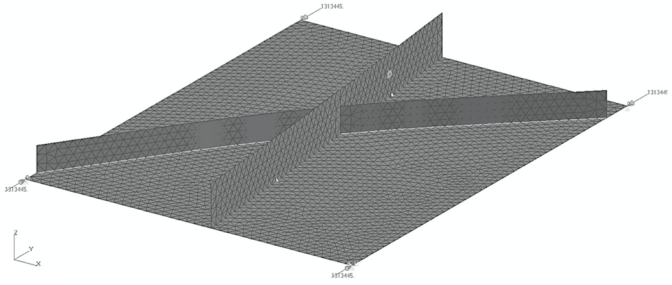

d) PSO-unified: 3.373 kg

Fig. 9 Comparison of optimum stiffener configurations for load case 1 (Tables 3 and 4.

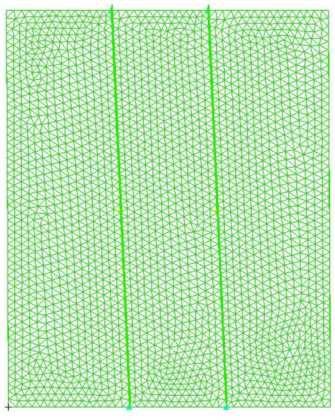

a) Stiffener effectiveness approach: 2.012 kg

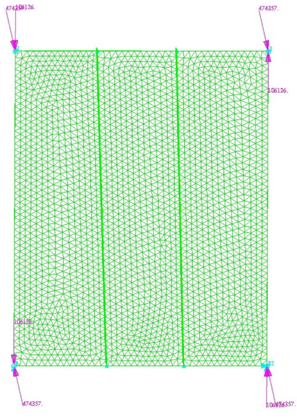

b) PSO-straight: 1.976 kg

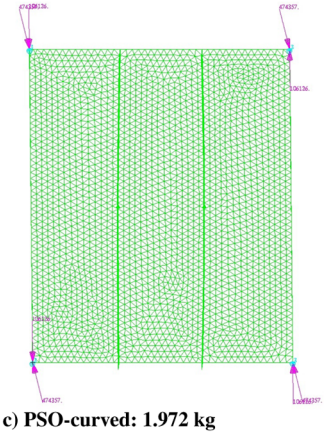

c) PSO-curved: 1.972 kg

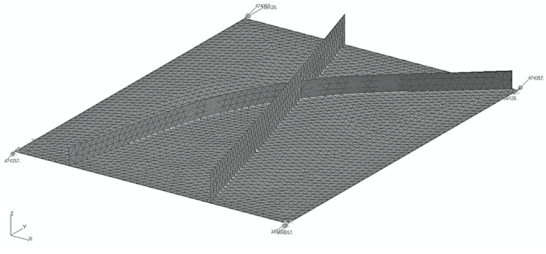

d) PSO-unified: 2.295 kg

Fig. 10 Comparison of optimum stiffener configurations for load case 2 (Tables 3 and 5.

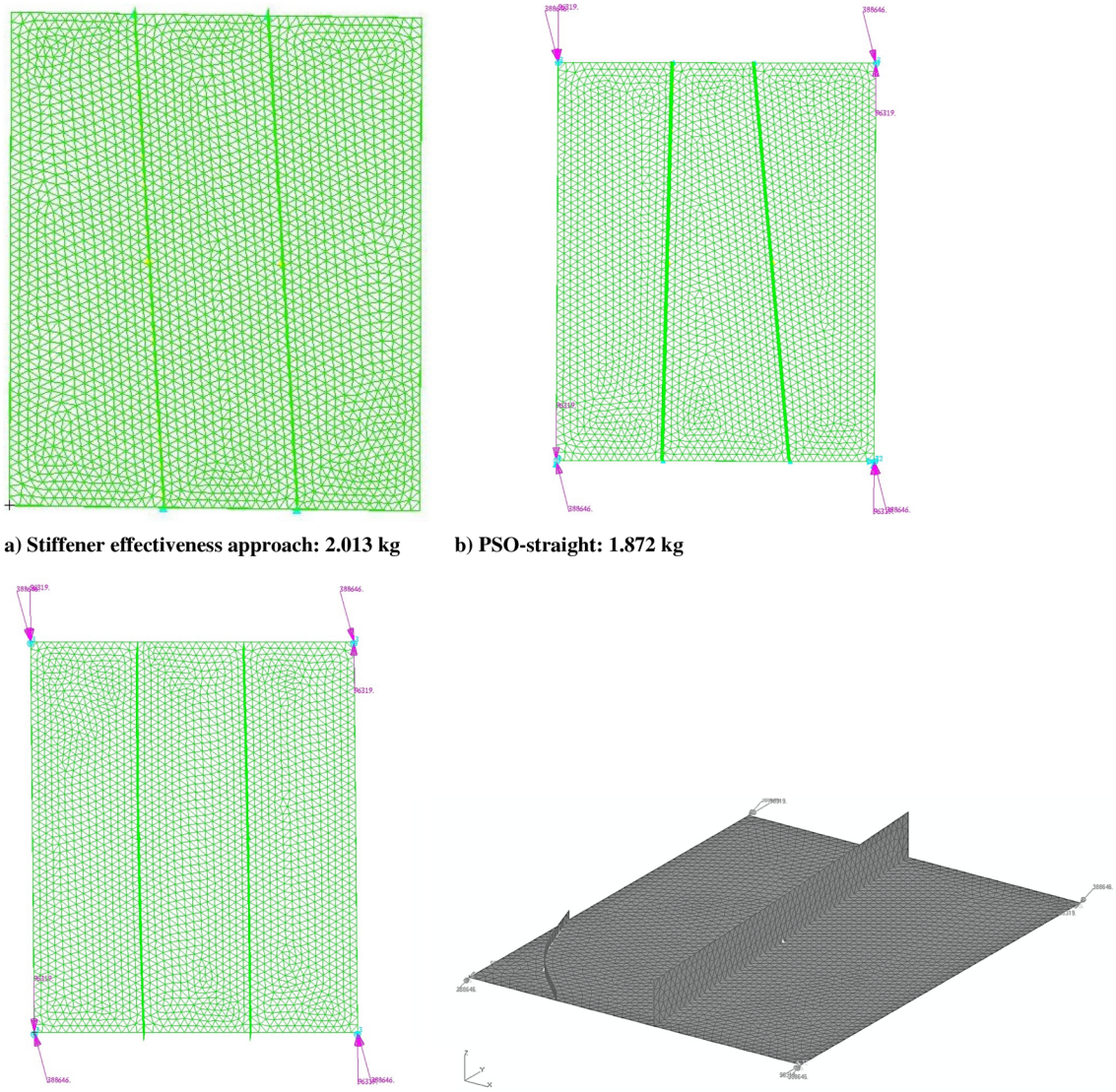

a) Stiffener effectiveness approach: 2.013 kg **b) PSO-straight: 1.872 kg**

c) PSO-curved: 1.832 kg **d) PSO-unified: 2.328 kg**

Fig. 11 Comparison of optimum stiffener configurations for load case 3 (Tables 3 and 6.

As mentioned earlier, the value of the metric is expected to give an idea of how effective a stiffener is in suppressing the buckling instability. Hence, a stiffener with a higher value of metric should result in a lower value of optimized mass or, in other words, the inverse of the metric is expected to have a similar variation as the optimum panel mass. This entirely depends on the quality of the metric definition.

For pure shear load case 1, the inverse of the two metrics is plotted against the stiffener orientation in Figs. 5b and 5c. The positive convention for stiffener orientation is shown in Fig. 3. The stiffener is kept straight, and the configurations for a few selected sets of orientations are shown on the top of each plot. Figure 5d is a plot of the optimized mass of the stiffened panel with respect to the stiffener orientation θ. This is obtained by holding the stiffener configuration fixed at the respective orientation and using an optimizer to find the stiffener and panel cross-sectional dimensions and the corresponding minimum mass. The buckling constraint is active for each configuration; hence, Fig. 5d is analogous to the curves presented in Figs. 5b and 5c. This plot is used as a reference for judging the quality of the two metrics.

A few observations are of interest here. First, it is seen from Fig. 5d that the point of maximum mass corresponds to $\theta = 45°$, which is correctly predicted by Fig. 5c. Additionally, the orientation for minimum mass is at $\theta = 22.5$ and $\theta = 112.5°$, which are closely approximated by Figs. 5b and 5c.

Similarly, for load case 2, with equal shear and compressive load magnitudes, the inverse of metrics are plotted in Figs. 6b and 6c, and the variation of optimized mass with stiffener orientation is shown in Fig. 6d. A comparison of the plots shows that, although the qualitative variation of the metric plots is similar to that of the mass variation, the locations of maximum and minimum mass predicted by the metrics are in slight disagreement. The two metrics predict the minimum mass to occur at around 100°, while the corresponding point in Fig. 6d occurs at around 93°.

For load case 3, which has a dominant compressive loading as compared with the shear loading, the corresponding plots are shown in Fig. 7. The inverse of the two metrics is plotted against θ in Figs. 7b and 7c. These predict the orientation for minimum mass to be around 95°, and the corresponding point from mass minimization is seen to occur in Fig. 7d at approximately 87°.

Finally, for load case 4 with a panel under uniaxial compression, the predicted locations of minimum mass from the metrics are at 90° (Figs. 8b and 8c), which is in agreement with that shown in Fig. 8d. For maximum mass, the predicted orientation of 0° also agrees with that seen in the variation of mass obtained from optimization.

These results suggest that a properly defined metric can be helpful in quick calculation of the best stiffener configuration for lowest mass of the panel subject to buckling loads. Both the metrics are seen to closely capture the stiffener orientations for maximum and minimum stiffened-panel mass subject to buckling constraints.

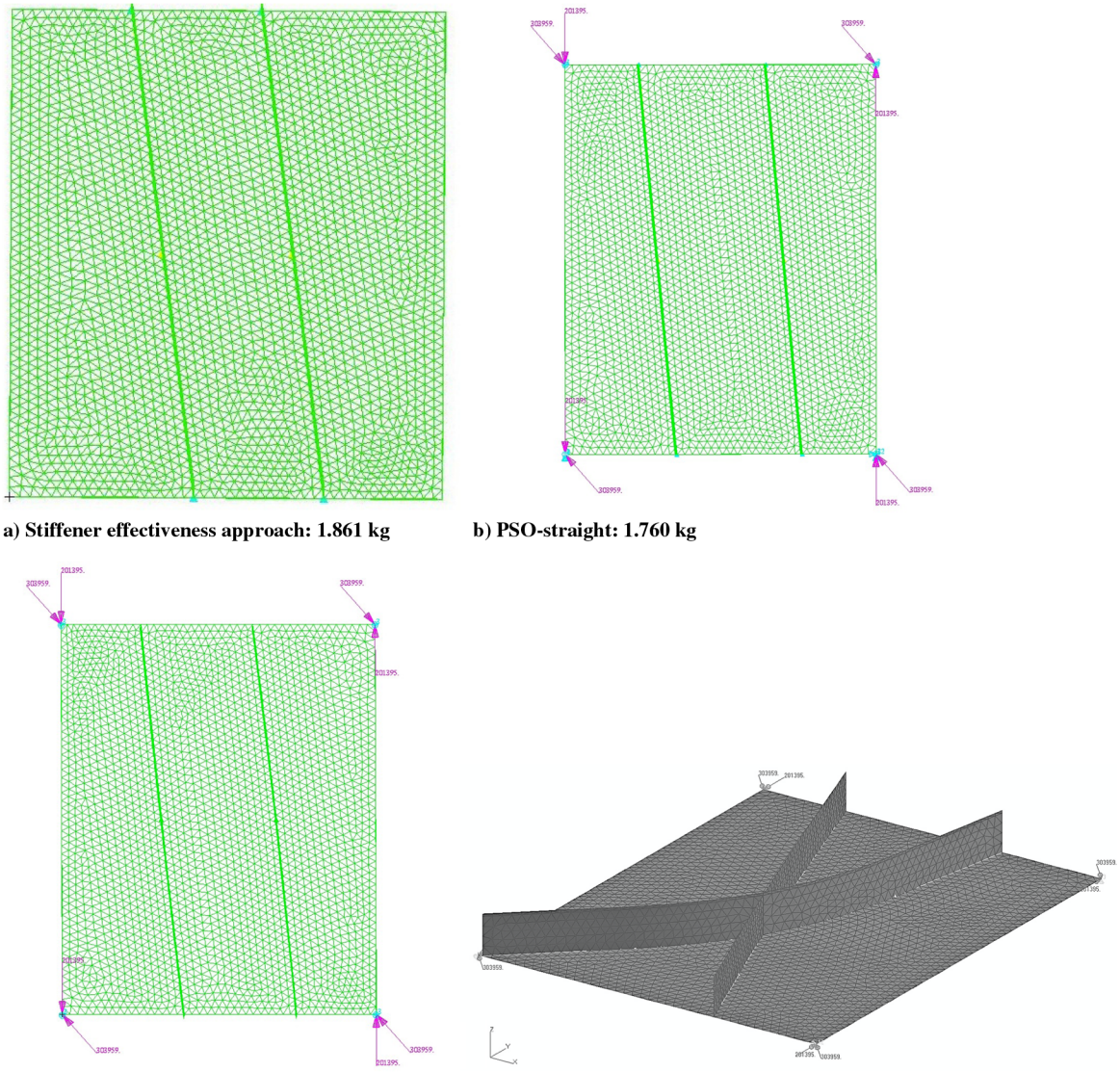

a) Stiffener effectiveness approach: 1.861 kg

b) PSO-straight: 1.760 kg

c) PSO-curved: 1.707 kg

d) PSO-unified: 1.970 kg

Fig. 12 Comparison of optimum stiffener configurations for load case 4 (Tables 3 and 7.

B. Simply Supported Rectangular Panel: Two Stiffeners

This section presents results for minimum mass optimization of a panel with two stiffeners. The material properties are listed in Table 1, and the design variables are listed in Table 2. Four different optimization approaches are studied:

1) As described in Sec. II.B.2, the SEA is used to find the stiffener curves. The effectiveness metric given in Eq. (10) is used in this study. This configuration is sized for minimum mass using gradient-based optimization. This approach works with only five design variables in the sizing optimization step. The optimization process in the SEA works with four design variables, which include the stiffener start and end points and the control point coordinates (points A, B, and C in Fig. 1), thereby allowing the stiffener to be curved.

2) The PSO-straight approach is a two-step optimization approach, described in Sec. II.B.3. The stiffener curves are kept straight, which reduce the number of design variables in the first step (shape optimization) to four, and reduce them to five in the second step (sizing optimization).

3) The PSO-curved approach is similar to the previous strategy, except the stiffeners are allowed to be curved.

4) The PSO-unified approach is the result of another set of results obtained using combined PSO and gradient-based optimization, where the optimum from PSO is used as a starting point for a gradient-based algorithm. This approach works with all 11 variables, with a total of 22 particles in PSO.

The load cases studied are listed in Table 3 along with the minimum mass and CPU time for each approach. The computations are performed on a computer with dual four-core 3.00 GHz Intel Xeon processors with 20 GB of RAM. Parallel processing is used for all cases, with eight simultaneous analyses. DAKOTA [22] is used for gradient-based optimization, while VisualDoc [23] is used for the results involving the PSO algorithm. The analyses are performed using EBF3PanelOpt [14]. The readers are referred to the paper by Gurav and Kapania [14] for a detailed description of the design variables.

The results in Table 3 show that the stiffener configurations obtained using the PSO-straight and PSO-curved approaches are very comparable to each other, except for load case 5. The exact CPU time for the PSO-curved approach was not available, but it was approximated based on the total number function evaluations and the time needed per evaluation. In most cases, this time is slightly higher than that for PSO-straight but significantly lower than the PSO-unified approach. This is typical of PSO, which needs far more function evaluations, as the dimensionality and design domain are increased. Additionally, the mass obtained from PSO-straight and PSO-curved are lower in comparison with the other two approaches (except load case 5). It is important to note that, although the mass obtained from SEA is slightly higher by 2 to 7%, the results take far less CPU time than the PSO-based approaches. This gives a strong validity to the effectiveness metric proposed in this paper.

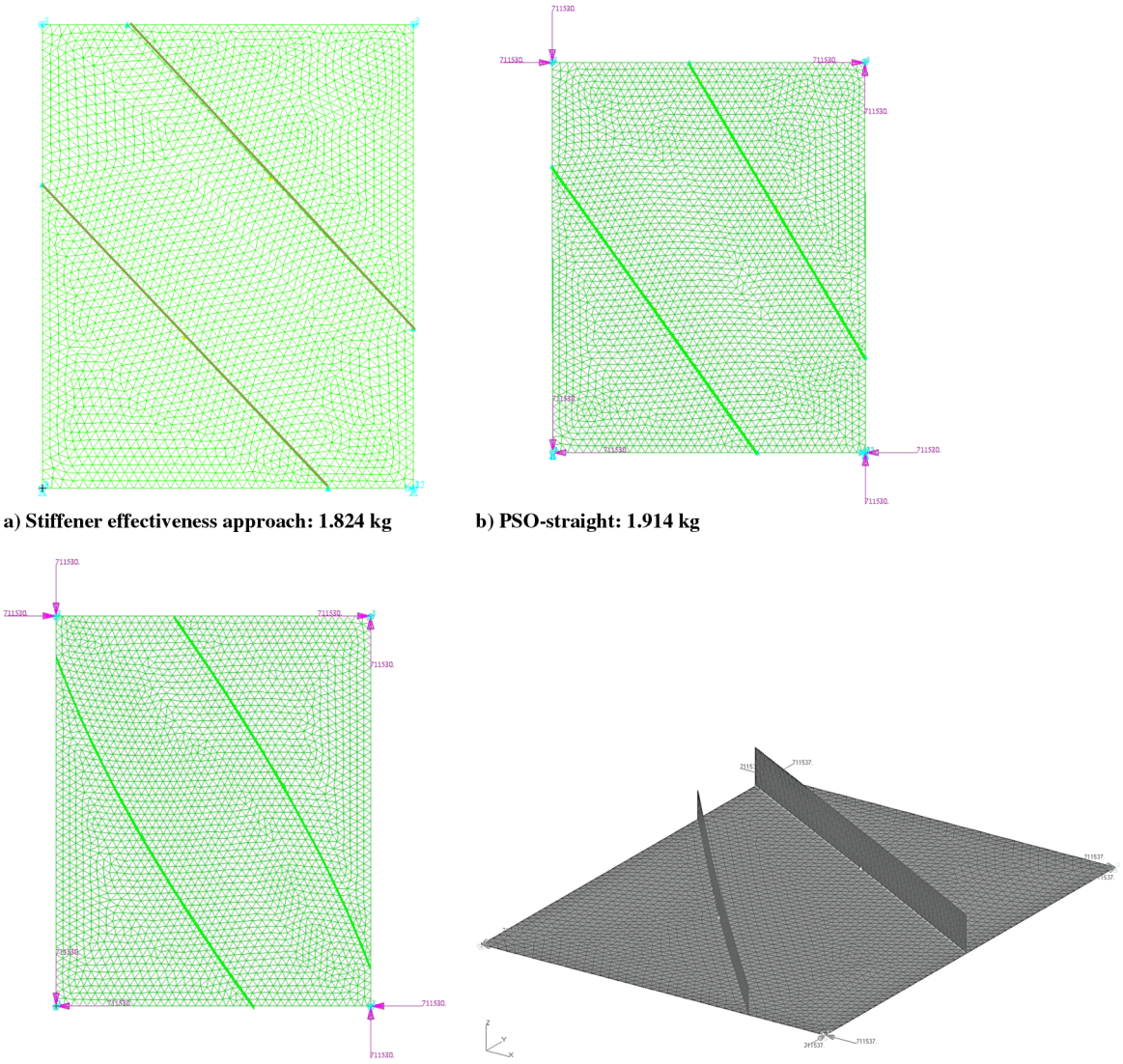

a) Stiffener effectiveness approach: 1.824 kg **b) PSO-straight: 1.914 kg**

c) PSO-curved: 2.151 kg **d) PSO-unified: 2.194 kg**

Fig. 13 Comparison of optimum stiffener configurations for load case 5 (Tables 3 and 8.

The optimum design variable values for each load case are listed in Tables 4–8, and the stiffener configurations from each approach are shown in Figs. 9–13. It should be noted that SEA allows the base stiffener curve to have a curvature, but the optimization procedure returns a straight stiffener. This is compared with the results obtained from PSO-curved approach.

For load case 1, the design variables are listed in Table 4, and the four stiffener configurations are shown in Fig. 9. The figures show the stiffened-panel geometry, with markers defining the panel loads that are uniformly distributed on the boundary. The SEA results in straight stiffeners oriented parallel to the longer edge of the panel (Fig. 9a), which is a similar orientation to the result obtained from PSO-straight (Fig. 9b). The stiffeners in PSO-straight are closer to each other than what is assumed for SEA, and they result in 3.8% lower mass. The configuration from PSO-curved (Fig. 9c) has curved stiffeners but practically the same mass as the PSO-straight design. This suggests that multiple designs with straight/curved stiffener designs exist with the same panel mass. The PSO-unified design, shown in Fig. 9d, is far from optimum and shows the challenge in obtaining reasonably converged designs using global optimizers in a unified design space.

The designs for load case 2, shown in Fig. 10 and listed in Table 5, show a similar trend. SEA results in straight stiffeners (Fig. 10a) that have a similar orientation to the PSO-straight design (Fig. 10b), which has a design lighter by only 1.8%. The PSO-curved (Fig. 10c) design has slightly curved stiffeners with a different orientation than the former two designs, but the mass is practically the same as that of PSO-straight. As for load case 1, this suggests the existence of multiple stiffener configurations with a very similar panel mass. The PSO-unified design is again far from optimum, highlighting the challenge of using global optimizers on a unified design space.

Load case 3 designs, shown in Fig. 11 and listed in Table 6, show that the PSO-straight and PSO-curved approaches result in designs that are very similar in mass but are lighter than the SEA design by about 7.3%. Although PSO-curved allows for curvature in the stiffener geometry, the optimization procedure returns a straight stiffener. The stiffener in the PSO-straight design has a different orientation than the other designs but a very similar mass to the PSO-curved. This again suggests that the design space has multiple designs with very similar panel mass. The PSO-unified design shows poor convergence.

Load case 4 results, in Fig. 12 (listed in Table 7), show similar trends, as in the previous load cases. It is important to note that the PSO-curved approach results in straight stiffeners, and the design is very similar to the PSO-straight configuration. These are lighter than the SEA design by 5.7%.

The load case 5 designs, in Fig. 13 and Table 8, show that the stiffeners from all four approaches are oriented in similar directions. However, the SEA design is the lightest of all approaches.

The poor optimizer convergence in PSO-unified is not well understood. The same optimizer convergence criteria is used as in the other cases. The maximum number of iterations is limited to 500,

while the relative convergence of objective function is limited to seven consecutive iterations. It appears that increasing the number of particles and the relative objective convergence iterations could have led to a better convergence behavior in this expanded design domain, but this would have come at a higher computational expense. Although the use of RSs could reduce this CPU expense, this would also be true for other PSO-based approaches.

IV. Conclusions

Design of stiffened panels with buckling constraints is a highly nonconvex optimization problem with multiple local minima. This makes the use of gradient-based optimizers very difficult, unless the starting point is in the vicinity of the optimum. Although global optimization algorithms can be used at a higher computational cost, our experience suggests that the highly nonconvex nature of the design space poses a challenge to their convergence.

This paper presents two new approaches toward optimal placement of stiffeners for minimum mass design of a stiffened panel. These are built on the heuristic concept of stiffener effectiveness, which argues that the most effective stiffener configuration leads to a panel with minimum mass. The problem then requires a way to find the most effective stiffener curve, and two approaches are proposed in this paper.

The first approach, called the SEA, proposes an effectiveness metric that uses the first buckling mode of the unstiffened panel and the applied loading. Two different metrics are proposed and studied, using a simple one-stiffener case under four different loading conditions. The results show that the metrics are able to closely predict the stiffener orientations of the maximum and the minimum panel mass. Although the metric is limited to one stiffener curve, a method is proposed to extend this to design two stiffeners. This is used to design stiffened panels with two stiffeners, and the results are compared with other approaches. It is seen that in significantly less CPU time, this method is able to design panels that are only 2–8% heavier than the other methods.

The second approach proposed in this paper decomposes the design variable space into two subspaces: one created by the sizing variables and the other with the shape variables. Separate optimization problems are solved in each subspace. The method is used to design two stiffened panels for five load cases: one where the stiffeners are kept straight, and the other where they are allowed to have a curvature. For three out of five load cases, the stiffeners obtained from the latter approach have close to zero curvature. The remaining two load cases have curved stiffeners. However, both methods design panels for which the masses are practically the same. This suggests that the design space has multiple designs with different stiffener configurations but very similar mass values.

Compared with optimization, results over a unified design space show that the proposed methods are able to design lighter panels in far less CPU time. It is, however, noted that in their present form, the methods are limited to design panels for a single load case. Additionally, the SEA assumes a uniformly applied load on the edges. These limitations can be overcome by modifications to the approach. For the two-step design approaches based on PSO, these limitations can be overcome by simply creating the stiffened-panel finite element model with a nonuniform load applied on the boundary.

Acknowledgments

The work presented here was funded under the NASA Subsonic Fixed Wing Hybrid Body Technologies NRA (NASA NN L08AA02C), with Karen Taminger as the Project Manager and Cynthia Lach and R. Keith Bird as the Contracting Officer's Technical Representatives. We are thankful to all of them for their suggestions. The authors would also like to thank our partners in the National Research Announcement project, Bob Olliffe, John Barnes, David Havens, and Steve Englestadt, and the Lockheed Martin Aeronautics Company of Marietta, GA, for technical discussions.

References

[1] Anderson, M. S., and Stroud, W. J., "General Panel Sizing Computer Code and its Application to Composite Structural Panel," *AIAA Journal*, Vol. 17, No. 8, 1979, pp. 892–897. doi:10.2514/3.61242

[2] Bushnell, D., "PANDA: Interactive Program for Minimum Weight Design of Stiffened Cylindrical Panels and Shells," *Computers and Structures*, Vol. 16, Nos. 1–4, 1983, pp. 167–189. doi:10.1016/0045-7949(83)90158-X

[3] Bushnell, D., "PANDA2: Program for Minimum Weight Design of Stiffened, Composite, Locally Buckled Panels," *Computers and Structures*, Vol. 25, No. 4, 1987, pp. 469–471. doi:10.1016/0045-7949(87)90267-7

[4] Bushnell, D., "Theoretical Basis of the PANDA Computer Program for Preliminary Design of Stiffened Panels under Combined In-Plane Loads," *Computers and Structures*, Vol. 27, No. 4, 1987, pp. 541–563. doi:10.1016/0045-7949(87)90280-X

[5] Williams, F. W., Anderson, M. S., Kennedy, D., Butler, R., and Aston, G., "User Manual for VICONOPT: An Exact Analysis and Optimum Design Program Covering the Buckling and Vibration of Prismatic Assemblies of Flat In-Plane Loaded, Anisotropic Plates, with Approximations for Discrete Supports, and Transverse Stiffeners," NASA CR 181966, 1990.

[6] Bushnell, D., Rankin, C. C., and Riks, E., "Optimization of Panels in which Mode Jumping is Accounted for," 38th AIAA/ASME/ASCE/AHS/ASC Structures, Structural Dynamics, and Materials Conference, Palm Springs, CA, AIAA Paper 1997-1141, 1997.

[7] Venkataraman, S., Lamberti, L., Haftka, R. T., and Johnson, T. F., "Challenges in Comparing Numerical Solutions for Optimum Weights of Stiffened Shells," *Journal of Spacecraft and Rockets*, Vol. 40, No. 2, 2003, pp. 183–193. doi:10.2514/2.3952

[8] "Hypersizer User's Manual," Ver. 5.4, Collier Research Corp., Hampton, VA, 2008.

[9] Bedair, O., "Analysis and Limit State Design of Stiffened Plates and Shells: A World View," *Applied Mechanics Reviews*, Vol. 62, No. 2, 2009, Paper 020801. doi:10.1115/1.3077137

[10] Luo, J., and Gea, H. C., "A Systematic Topology Optimization Approach for Optimal Stiffener Design," *Structural optimization*, Vol. 16, No. 4, 1998, pp. 280–288. doi:10.1007/BF01271435

[11] Ding, X., and Yamazaki, K., "Stiffener Layout Design for Plate Structures by Growing and Branching Tree Model (Application to Vibration-Proof Design)," *Structural and Multidisciplinary Optimization*, Vol. 26, Nos. 1–2, 2004, pp. 99–110. doi:10.1007/s00158-003-0309-4

[12] Hyer, M., and Lee, H., "The Use of Curvilinear Fiber Format to Improve Buckling Resistance of Composite Plates with Central Circular Holes," *Composite Structures*, Vol. 18, No. 3, 1991, pp. 239-261. doi:10.1016/0263-8223(91)90035-W

[13] Setoodeh, S., Abdalla, M., and Gurdal, Z., "Design of Variable-Stiffness Laminates Using Lamination Parameters," *Composites Part B: Engineering*, Vol. 37, Nos. 4–5, 2006, pp. 301–309. doi:10.1016/j.compositesb.2005.12.001

[14] Gurav, S., and Kapania, R. K., "Development of Framework for the Design Optimization of Unitized Structures," 50th AIAA/ASME/ASCE/AHS/ASC Structures, Structural Dynamics, and Materials Conference, Palm Springs, CA, AIAA Paper 2009-2186, 4–7 May 2009.

[15] Kapania, R. K., Li, J., and Kapoor, H., "Optimal Design of Unitized Panels with Curvilinear Stiffeners," AIAA 5th Aviation, Technology, Integration, and Operations Conference (ATIO)/16th Lighter-than-Air and Balloon Systems Conference, Arlington, VA, AIAA Paper 2005-7482, 26–28 Sept. 2005.

[16] Mulani, S. B., Li, J., Joshi, P., and Kapania, R. K., "Optimization of Stiffened Electron Beam Freeform Fabrication (EBF3) Panels Using Response Surface Approaches," 48th AIAA/ASME/ASCE/AHS/ASC Structures, Structural Dynamics, and Materials Conference, Honolulu, HI, AIAA Paper 2007-1901, 23–26 April. 2007.

[17] Joshi, P., Mulani, S. B., Kapania, R. K., and Shin, Y., "Optimal Design of Unitized Structures with Curvilinear Stiffeners Using Response Surface Methodology," 49th AIAA/ASME/ASCE/AHS/ASC Structures, Structural Dynamics, and Materials Conference, Schaumburg, IL, AIAA Paper 2008-2304, 7–10 April 2008.

[18] Wang, C. Y., and Wang, C. M., "Buckling of Circular Plates with an Internal Ring Support and Elastically Restrained Edges," *Thin-Walled*

Structures, Vol. 39, No. 9, 2001, pp. 821–825. doi:10.1016/S0263-8231(01)00031-3

[19] Barik, M., "Finite Element Static, Dynamic and Stability Analyses of Arbitrary Stiffened Plates," Ph.D. Thesis, Department of Ocean Engineering and Naval Architecture, Indian Inst. of Technology Kharagpur, India, 1999.

[20] Farin, G., *Curves and Surface For CAGD: A Practical Guide*, 5th ed., Morgan Kaufmann, San Mateo, CA, 2002.

[21] Venter, G., and Sobieski, J. S., "Particle Swarm Optimization," *AIAA Journal*, Vol. 41, No. 8, 2003, pp. 1583–1589. doi:10.2514/2.2111

[22] Eldred, M. S., Adams, B. M., Gay, D. M., Swiler, L. P., Haskell, K., Bohnhoff, W. J., Eddy, J. P., Hart, W. E., Watson, J. P., Hougn, P. D., and Kolda, T. G., "DAKOTA, A Multilevel Parallel Object-Oriented Framework for Design Optimization, Parameter Estimation, Uncertainty Quantification, and Sensitivity Analysis," Sandia National Labs., Paper SAND2006-6337, Albuquerque, NM, Oct. 2006, Livermore, CA.

[23] "VisualDoc User's Manual," Ver. 6.2, Vanderplaats Research and Development, Colorado Spring, CO, Aug. 2009.